

An Experimental Approach for Condition Monitoring of Magnetic Cores with Grain Oriented Electrical Steels

Hamed Hamzehbahmani, *Senior member, IEEE*
 Department of Engineering, Durham University, Durham, DH1 3LE, UK

Abstract- This paper proposes a new approach to an old challenge in the magnetic cores of power transformers and other magnetic devices with grain oriented electrical steels. The main aim of this paper is to evaluate effects of inter-laminar faults of different configurations on dynamic performance and dynamic energy losses of the magnetic cores with grain oriented silicon steels. In the relevant studies, artificial short circuits of different configurations were applied between the laminations of stacks of four Epstein size laminations of 3 % grain oriented silicon steel. The results showed that, inter-laminar fault evaluation and core quality assessment can be effectively done by interpreting the dynamic hysteresis loops of the cores.

Index Terms: Condition monitoring, transformer core, soft magnetic material, dynamic hysteresis loop, magnetic loss, dynamic modelling.

I. INTRODUCTION

Electrical steels are key materials for magnetic cores of reactors, transformers and electrical machines. Quality of the magnetic cores are determined by electrical and magnetic properties of the magnetic materials, coating of the laminations which determine the inter-laminar resistance between the laminations, clamping pressure, manufacturing processes, etc. Key amongst these are manufacturing processes which have direct impacts on properties of the materials and hence normal operation of the magnetic cores and related devices [1-7].

Magnetic and electric properties of the individual laminations and the assembled cores can be deteriorated by manufacturing processes, e.g. cutting, punching, stamping and welding, as a result of mechanical and thermal residual stress [7]. Additionally, punching and cutting could lead to microscopic edge burrs around the punched holes or at the cut edge, and can cause low inter-laminar resistance, electrical contact and hence inter-laminar fault (ILF) between the laminations [2], [8-12]. ILF leads to circulating eddy currents between the defective laminations, which cause hot spot and extra localised power loss at the defective zone. A few faults may not create high ILF currents; but with several faults, the induced fault currents could be large and cause excessive local heating in the damaged area [5-6]. Though a large number of ILF could result in catastrophic breakdown, the machine can still be in operation with a small number of ILF, but with higher power loss and hence lower efficiency. Local power losses and hot spots in the magnetic cores, could expedite the degradation of the coating material of the laminations and result in deterioration of the core at early stages. Therefore, condition monitoring of the magnetic cores to identify any ILF should be planned at an early stage before it progresses to machine breakdown. Examples of ILF in a three-phase three-limb transformer core are shown in Fig 1. Side view of a stack of grain oriented (GO) 3 % silicon steel laminations with ILF between two laminations is shown in Fig 2 [1].

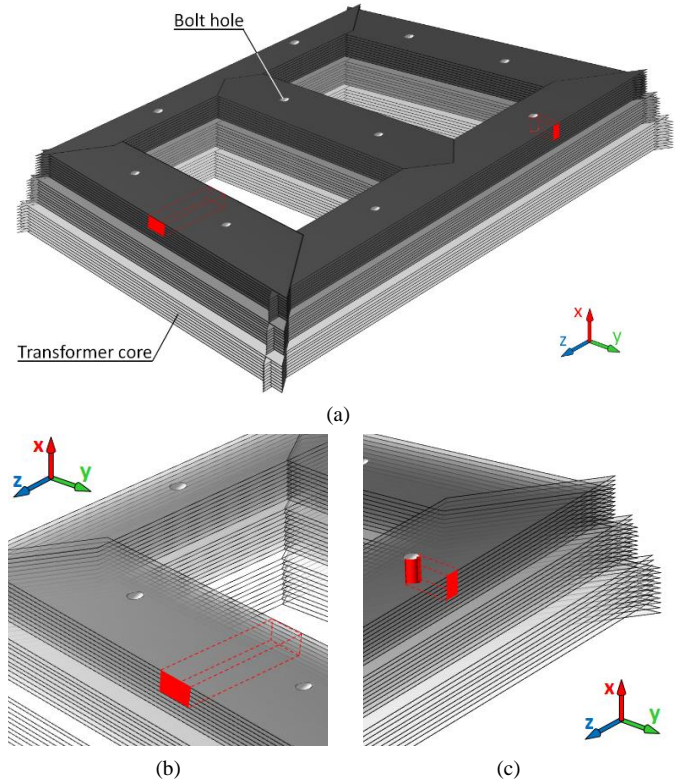


Fig 1 Perspective view of a three-phase three-limb transformer core with ILFs (a) Overall view (b) ILF between bolt hole and yoke and (c) ILF on two sides of the limb

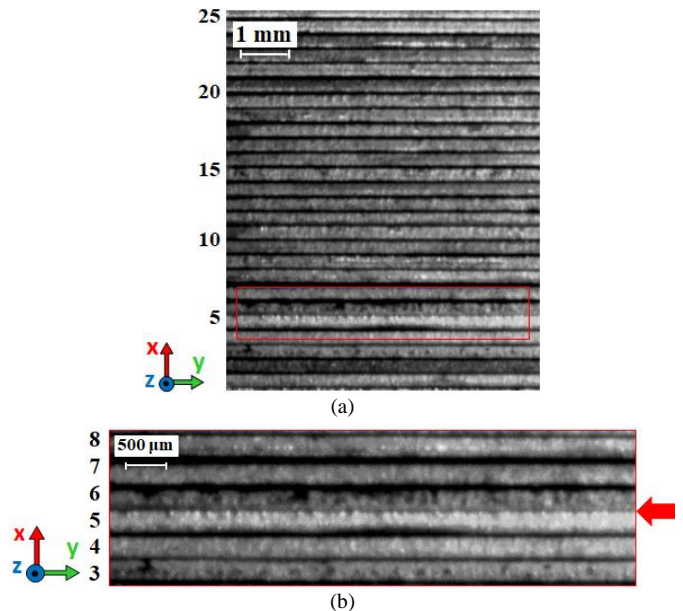


Fig 2 A stack of 3 % grain oriented silicon steel with ILF between two laminations [1]

ILF detection and condition monitoring of the magnetic cores have been an active area of research and interesting topic for designers and manufacturers of the electrical steels and laminated magnetic cores. In this regards, practical methods have been introduced and successfully employed to evaluate ILF of rotating machines [4-12] and transformers [13-16], and other magnetic devices with laminated cores. An overall review of these methods is performed in [1].

Electrical steels are characterised by the relative permeability and specific power loss in W/kg or total energy loss in J/m³ during one magnetising cycle. Data sheets from the steel manufacturers typically report the specific loss figure of the materials measured at power frequencies, 50 Hz or 60 Hz, for selected peak flux densities. Specific power loss published in the data sheets of the material, however, do not count for the geometry of the magnetic cores, and degradation of the material due to manufacturing processes. Furthermore, it is well distinguished that low inter-laminar resistance in the clamped magnetic cores due to, for example, edge burr or damage on the surface coating has a significant impact on the local and overall power loss of the magnetic cores [15-16]. Therefore, designers of the electrical machines and transformers usually find considerable deviation between the measurements of single lamination and overall power losses measured from the assembled cores.

The main aim of this paper is to evaluate magnetic cores of GO materials by measuring and interpreting the Static Hysteresis Loop (SHL) and Dynamic Hysteresis Loop (DHL) of the core. The measurements were performed on stacks of four Epstein size laminations of GO silicon steel subjected to artificial ILF of different configurations. A new approach has been also developed to reproduce DHLs of the samples under sinusoidal induction with magnetising frequency of 50 Hz and peak flux densities of 1.3 T, 1.5 T and 1.7 T. This method can be used to evaluate the impacts of typical ILFs on the dynamic performance and dynamic energy loss of power transformers and other magnetic devices with GO materials.

II. THEORETICAL BASE

Magnetising process of the magnetic materials can be analysed by means of the hysteresis phenomenon. The area surrounded by the hysteresis loop represents the total energy loss per unit volume for one magnetising cycle, in J/m³ per cycle. Accurate measurements of SHL and DHL, is an adequate technique of loss evaluation of magnetic materials over a wide range of magnetisation. However in these analyses, different approaches might be applied for different materials. In this regard, analytical methods have been developed to reproduce DHLs of the materials for energy loss prediction and separation [17-23].

A perspective view of a single lamination of thickness d subjected to flux density $B(t)$ applied in rolling direction (z -direction) is shown in Fig 3. If eddy current loops are assumed to be large enough along the y -direction, the field problem becomes one dimensional and the magnetisation process of the material can be evaluated for z -component of the magnetic flux density $B_z(x, t)$ by numerical solution of the well-known 1-D diffusion equation [20]:

$$\frac{\partial B_z(x, t)}{\partial t} = \rho \frac{\partial^2 H_z(x, t)}{\partial x^2} \quad (1)$$

which links the flux density $B_z(x, t)$ and the field strength $H_z(x, t)$ in a thin ferromagnetic lamination of resistivity ρ . It should be noted that (1) is a Maxwell equation describing diffusion process in a spatially homogeneous medium.

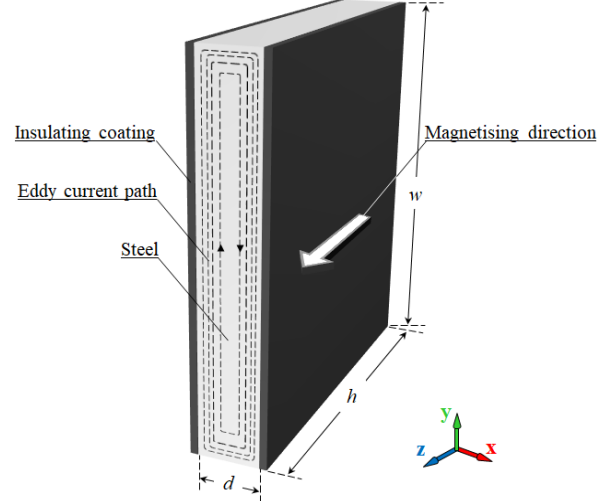


Fig 3 Single strip lamination under time varying magnetic field

Due to the approximate homogeneous nature of Non-Oriented (NO) steels, (1) can be implemented to characterise NO steels, with reasonable accuracy [20]. However, loss calculation of GO steels by means of (1) results in a significant discrepancy with the measured values. Numerical solution of (1) has been modified to characterise GO steels, by taking into account an accurate static hysteresis model, skin effect and correction factors [24]. Although the achievements are somehow satisfactory, but due to inhomogeneous nature and grain structure of the GO materials, the developed models based on (1) cannot be extended for all types of GO steels, especially for high frequency magnetisations and high permeability materials. An alternative approach to evaluate the magnetisation process of GO materials is thin sheet model, which is based on the statistical energy loss separation principle [17]. In this approach, the total energy loss W_{tot} , is separated into three components, hysteresis loss W_{hys} , classical eddy current loss W_{eddy} , and anomalous loss or excess loss W_{exc} [17]:

$$W_{tot} = W_{hys} + W_{eddy} + W_{exc} \quad (2)$$

Energy loss calculation and separation can be performed based on the static and dynamic hysteresis loops of the material, and therefore, loss separation of (2), can be interpreted as magnetic field separation:

$$H(t) = H_{hys} + H_{eddy} + H_{exc} \quad (3)$$

where $H(t)$ is the magnetic field at the surface of the lamination, H_{hys} is hysteresis field, H_{eddy} is eddy current field, and H_{exc} is excess field. Using the dynamic models of H_{eddy} and H_{exc} , (3) led to the well-known thin sheet model and is expressed as [19]:

$$H(t) = H_{hys}(B) + \frac{d^2}{12\rho} \frac{dB}{dt} + g(B)\delta \left| \frac{dB}{dt} \right|^\alpha \quad (4)$$

where $H_{hys}(B)$ is the hysteresis field, d is thickness of the material and $\delta = \text{sign}(dB/dt)$ is directional parameter for ascending ($dB/dt > 0$) and descending ($dB/dt < 0$) hysteresis branches. The exponent α determines the frequency law of the excess loss component calculated by (4) under sinusoidal induction. $g(B)$ is an important function which control shape of the dynamic hysteresis loop. Accuracy of the calculated loss depends on the accuracy of the dynamic hysteresis loop, reproduced by the dynamic model of (4), which mainly depends on the hysteresis field $H_{hys}(B)$ and function $g(B)$. Examples of calculating $g(B)$ for some commercial materials are provided in [21]. Recent publications show high accuracy of model (4) in characterisation of GO steels [19-20], and some high silicon NO steels [18].

Energy loss separation can be also interpreted by separating the total energy loss into hysteresis and dynamic components. In this method, both classical eddy-current and excess fields are interpreted as dynamic field, and hence loss separation and field separation can be expressed as [25]:

$$W_{tot} = W_{hys} + W_{dyn} \quad (5)$$

$$H(t) = H_{hys}(B) + H_{dyn}(t) \quad (6)$$

where $H_{hys}(B)$ is the hysteresis field and W_{hys} is the area of the static, or quasi-static hysteresis loop. Based on the two terms energy loss, a dynamic model is proposed in [20] for GO materials as follow:

$$H(t) = H_{hys}(B) + g_{dyn}(B)\delta \left| \frac{dB}{dt} \right|^{\alpha_{dyn}(B_{pk})} \quad (7)$$

where $g_{dyn}(B)$ and $\alpha_{dyn}(B_{pk})$ differ from $g(B)$ and α in (4). This model shows a good accuracy to reproduce the DHL of GO materials and hence energy loss calculation [20, 21]. It should be noted that, accuracy of the model (7) to reproduce the DHL, energy loss prediction and energy loss separation depends on the accuracy of the measured or calculated hysteresis field $H_{hys}(B)$ and the designed functions for $g_{dyn}(B)$ and $\alpha_{dyn}(B_{pk})$.

It has been shown that ILFs have significant impacts on the dynamic behaviour of the magnetic cores [26]. Therefore, in this paper model (7) was implemented to reproduce the DHLs of stacks of laminations of GO steels, subjected to ILFs.

III. EXPERIMENTAL SET-UP AND SAMPLE PREPARATION

Epstein size laminations (30 mm × 305 mm) with standard grades of M105-30P CGO 3 % SiFe (thickness $d = 0.3$ mm and resistivity $\rho = 0.461 \mu\Omega\text{m}$) were provided by Cogent Power Ltd. Stacks of four laminations were prepared to model different types of ILFs. The stacks were labelled as: Pack # 1, Stack of laminations with no ILF; Pack # 2, ILFs at three step-like points; Pack # 3, ILFs at one set point and Pack # 4, ILFs at three set points. Similar to the previous work [2], partial artificial faults of 10 mm wide and $\sim 500 \mu\text{m}$ thick were applied between the

laminations. Based on a study performed in [2], lead-free solder was found as an effective material to reproduce effect of ILF in clamped magnetic cores. Side view and top view of one the artificial faults is shown in Figs 4-a and 4-b, respectively. Perspective view of the samples are shown in Fig 5.

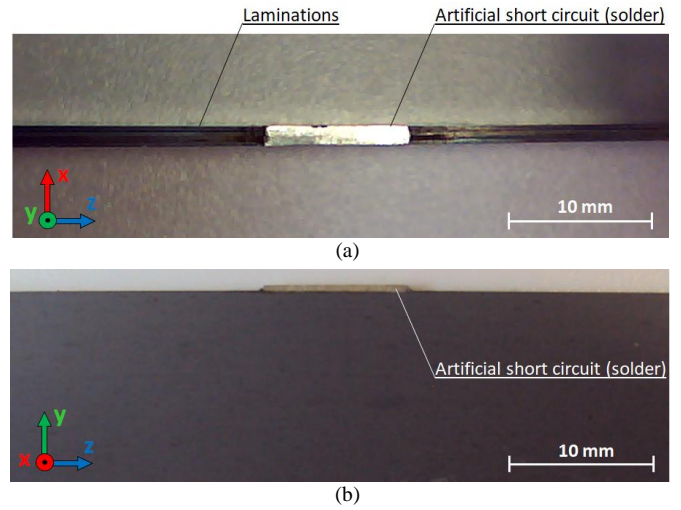


Fig 4 Artificial fault applied on the samples (a) side view and (b) top view

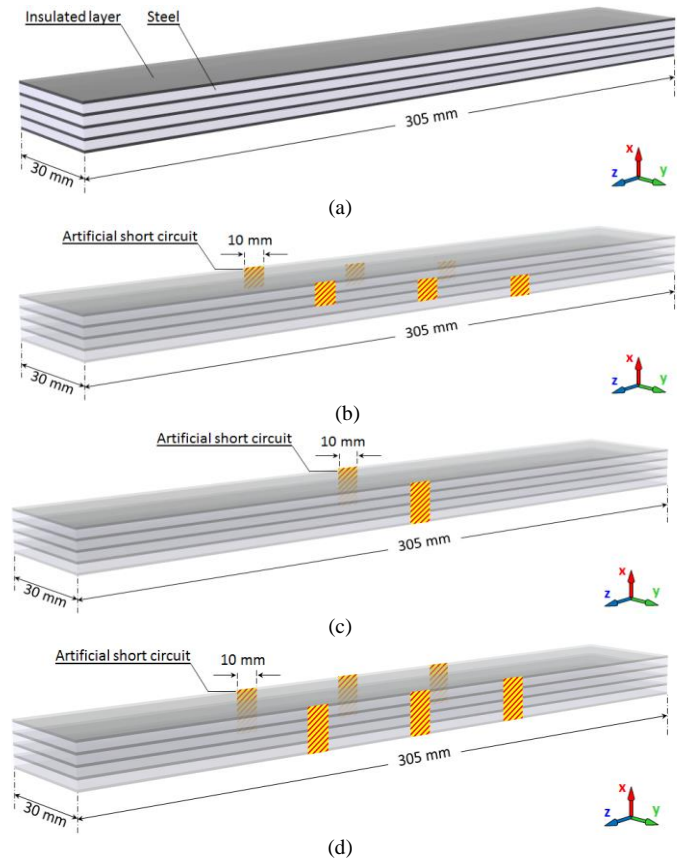


Fig 5 Perspective view of stacks of four laminations (a) without ILF (pack # 1); and with ILFs (b) at three step-like points (pack # 2) (c) one set point (pack # 3) and (d) at three set points (pack # 4)

Electrical steels are usually characterised at flux densities close to the knee of the B - H curve. Electrical steel manufactures

also provide the specific power loss of the materials typically at peak flux densities of 1.5 T and 1.7 T, and power frequency of 50 Hz or 60 Hz. Furthermore it has been shown that, at each particular frequency, ILF problems become more crucial at higher flux densities [2]. In this work a standard double yoke single strip tester (SST) was used to magnetise the samples under sinusoidal induction at peak flux densities of 1.3 T, 1.5 T and 1.7 T and magnetising frequency of 50 Hz. The measuring system conforms to the British standard BS EN 10280:2007. This system shows good reproducibility of measurements for a wide range of frequency and flux density. The reproducibility of this system is characterised by a relative standard deviation of 1 % for GO materials and of 2 % for NO materials [27]. More detail of the experimental setup is available in [24].

IV. EXPERIMENTAL RESULTS

SHL, DHL and total energy losses of the samples were measured and analysed for quality assessment purposes. DHL and total energy loss of pack # 1, with no ILF, represent the nominal qualities of the material. A comparison between the DHLs of the specimens at peak flux densities of 1.7 T, 1.5 T and 1.3 T are shown in Fig 6. The most evident feature of the DHLs of Fig 6 is the change in the hysteresis loop shapes and significant increase in the loop area for different types of ILFs. As stated earlier, with increasing ILFs the induced ILF currents increase which result in larger loop area in the DHLs and hence higher energy loss. However, the experimental results showed that SHLs of the samples are almost indistinguishable from each other. Therefore it could be concluded that, the ILFs have a significant impact on the dynamic energy losses, while their impact on the hysteresis energy losses is negligible. This reflects a unique property of the hysteresis phenomenon in energy loss evaluation, which can be implemented in the characterisation of the magnetic cores of transformers, electrical machines and other magnetic devices with laminated cores. This is a powerful technique in core quality assessment and can provide a meaningful comparison between magnetic properties of the magnetic cores subjected to different types of ILFs.

Total energy loss of the samples versus peak flux density are shown in Fig 7. Total energy loss of each pack was measured three times at each flux density with repeatability of better than 0.3 %. Experimental results presented in this paper are the average of three measurements. The estimated uncertainty of the measurements are shown by error bars [28]. The measured values lie within the upper and lower limits of the error bars. The extra energy loss caused by the ILFs on pack # 2 to pack # 4 were calculated as the difference between the energy loss of each pack and that of pack # 1; the results are shown in Fig 8. The results show that, the lowest increase in total energy loss is 15.1 % for pack # 2 at peak flux density of 1.3 T. Under the same magnetising condition, percentage increase in the total energy loss of pack # 4 is 66.6 %. The highest loss increase was observed for pack # 4 at peak flux density of 1.7 T, which is 76.6 %. In the IEEE standard 62.2-2004 [29] it is recommended that ILFs, which result in 5 % increase in total core loss (or result in a hot spot 10° C above the ambient after 2 hours test), should be identified as critical fault. The experimental results showed

that, even a few ILFs under power frequency magnetisation and a low flux density of 1.3 T, could lead to critical hot spot in the magnetic cores. This shows the importance of the ILFs in quality of the magnetic cores. More analysis on the bulk power loss of the samples over a wide range of frequency and flux density is provided in [2].

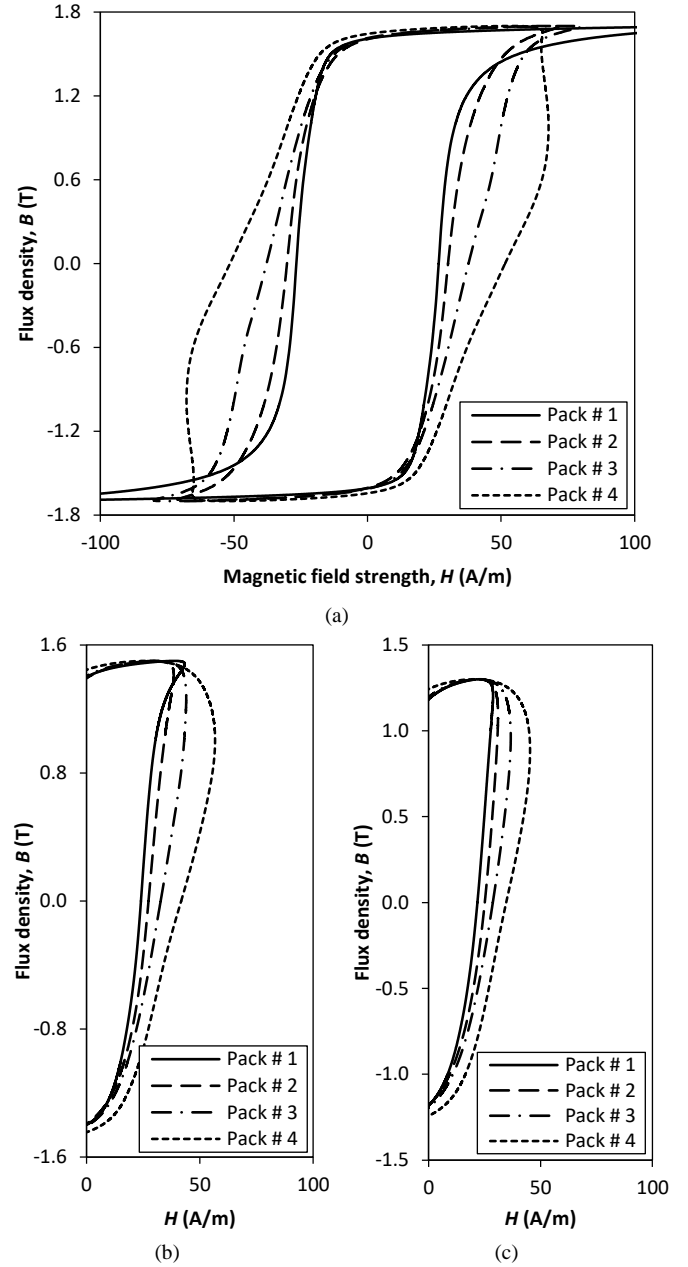


Fig 6 DHL of the samples under sinusoidal induction at frequency of 50 Hz and peak flux densities of (a) $B_{pk}=1.7$ T (b) $B_{pk}=1.5$ T and (c) $B_{pk}=1.3$ T

From (5) the area between the static and dynamic hysteresis loops, corresponding to the second term of model (7), represents the dynamic energy loss per cycle (W_{dyn}). The dynamic energy loss per cycle was calculated for each sample for the range of flux densities. Ratio of the dynamic energy loss to the total energy loss was also calculated. The results are shown in Figs 9-a and 9-b, respectively.

Fig 9 shows that for pack # 1, with no ILF, the dynamic energy loss counts for about 50 % of the total energy loss, for all flux densities. However, dynamic energy losses are increased to about 55 %, 65 % and 72 % for pack # 2, pack # 3 and pack # 4, respectively. This proves the initial conclusion that, ILFs have a direct impact on the dynamic energy loss of the magnetic cores.

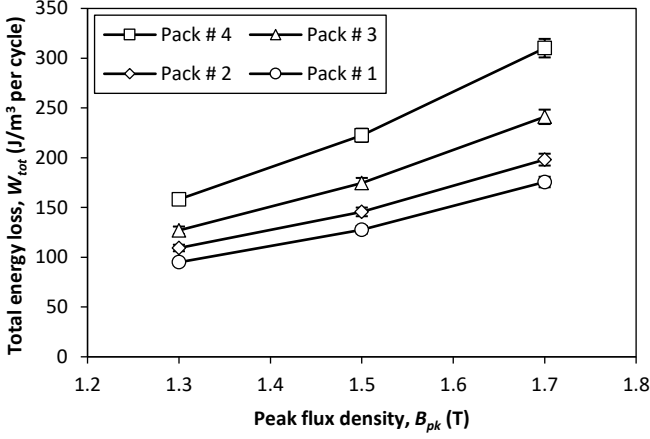


Fig 7 Total energy loss of the samples

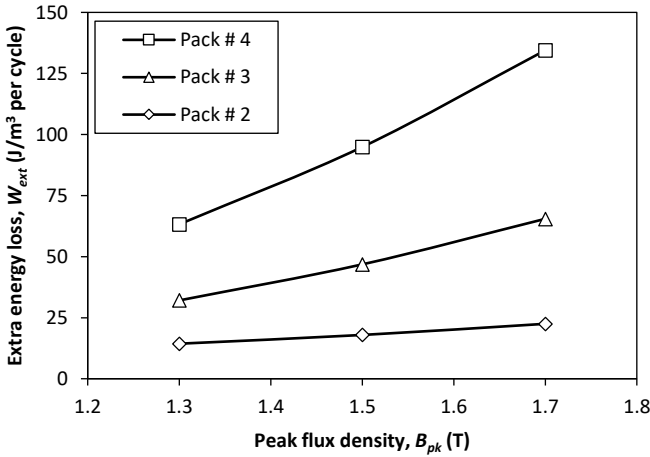


Fig 8 Extra energy losses of pack # 2 to pack # 4

V. MODELLING RESULTS

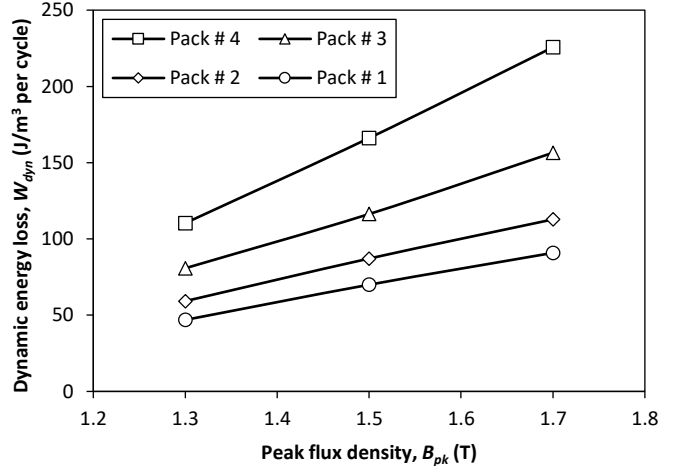
DHLs of the samples were reproduced using model (7). Based on a trial-and-error method, it was found that a constant exponent of $\alpha_{dyn}(B_{pk}) = 0.57$ is acceptable for all samples and flux densities. Function $g_{dyn}(B)$ was constructed for each portion of the measured DHLs to coincide the calculated and measured loops. Due to the distinct shape of the DHLs of pack # 2 to pack # 4, function $g_{dyn}(B)$ was found considerably different, and more complicated, than that for pack # 1. The following computational functions for $g_{dyn}(B)$ were found acceptable at a peak flux density of $B_{pk}=1.7$ T for pack # 1 to pack # 4, respectively.

$$g_{dyn1}(B) = \begin{cases} 0.5(1 + 0.2 B^2) & -1.7 < B < 0 \\ 0.46 - 0.18B & 0 < B < 1.7 \end{cases} \quad (8)$$

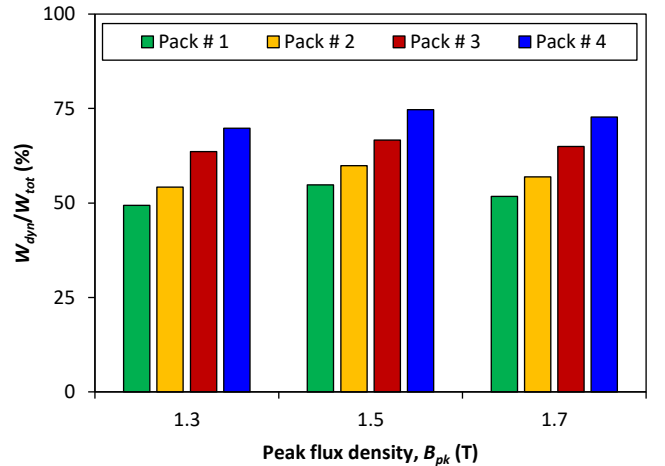
$$g_{dyn2}(B) = \begin{cases} 0.64 & -1.7 < B < -0.5 \\ 0.60 - 0.08B & -0.5 < B < 0.7 \\ 0.55 & 0.7 < B < 1.4 \\ -25.3 + 12B(3 - B) & 1.4 < B < 1.7 \end{cases} \quad (9)$$

$$g_{dyn3}(B) = \begin{cases} 0.75 & -1.7 < B < 0.3 \\ 0.72 - 0.18B(B - 1.4) & 0.3 < B < 1.4 \\ -13.4 - 7.4B(B - 2.8) & 1.4 < B < 1.7 \end{cases} \quad (10)$$

$$g_{dyn4}(B) = \begin{cases} 0.65(1 + 0.1 B^2) & -1.7 < B < -1.0 \\ 0.98 + 0.11B(B + 3.3) & -1.0 < B < 0.4 \\ 0.87 - 0.66B(B - 1.4) & 0.4 < B < 1.4 \\ -12.4 - 7.3B(B - 2.7) & 1.4 < B < 1.7 \end{cases} \quad (11)$$



(a)



(b)

Fig 9 (a) Dynamic energy loss of the samples (b) Ratio of the dynamic energy loss to the total energy loss

The measured and calculated DHLs of pack # 1 to pack # 4 under sinusoidal induction at magnetising frequency of 50 Hz and a peak flux density of $B_{pk}=1.7$ T are shown in Figs 10-a to 10-d, respectively. For comparison, the measured SHLs of the samples, which represents the hysteresis energy loss, are shown for each sample.

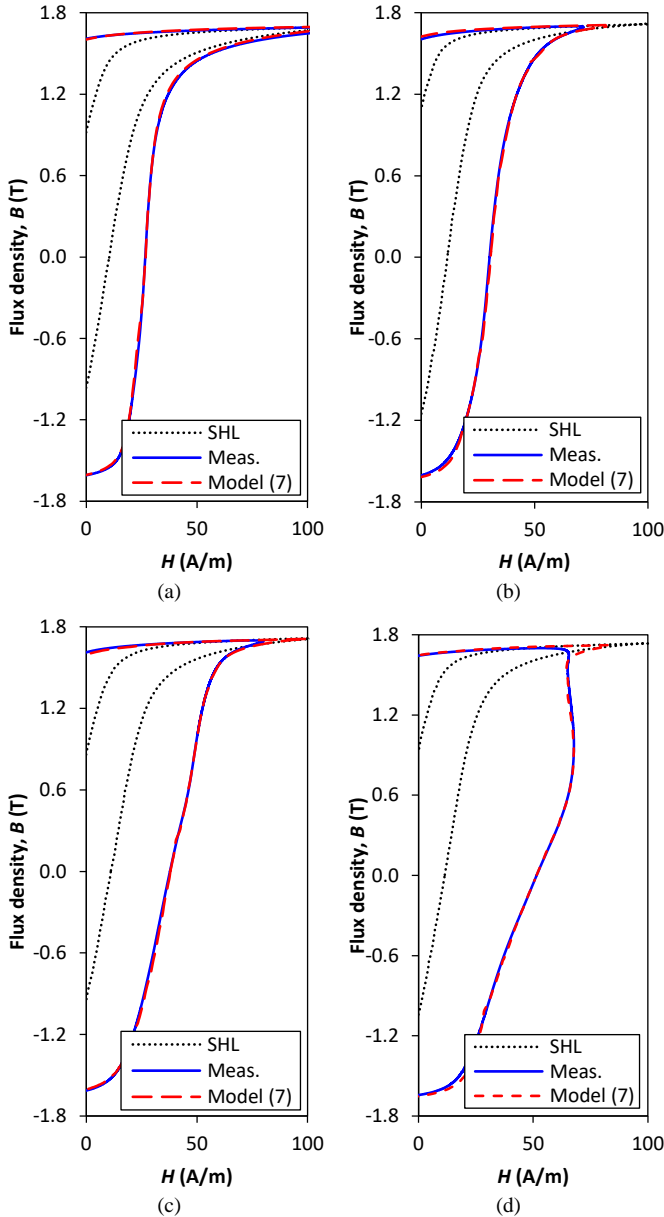


Fig 10 Comparison between the measured and modelled DHLs at peak flux density of $B_{pk}=1.7$ T (a) pack # 1 (b) pack # 2 (c) pack # 3 and (d) pack # 4

As can be seen from Fig 10, model (7) grants a fairly accurate basis to calculate the DHLs of the samples by which the total energy loss can be calculated. The same procedure as for peak flux density of $B_{pk}=1.7$ T was implemented to calculate the DHLs at peak flux densities of $B_{pk}=1.3$ T, $B_{pk}=1.5$ T. A comparison between the calculated and measured DHLs at magnetising frequency of 50 Hz and peak flux densities of $B_{pk}=1.3$ T, $B_{pk}=1.5$ T and $B_{pk}=1.7$ T are shown in Figs 11-a to 11-d, respectively.

Fig 11 shows that the calculated DHLs coincide with the measured loops for the range of measured flux density. Total energy losses per cycle from the modelled and measured DHLs were calculated for all samples and flux densities. A comparison between the results and the percentage difference between the values are shown in Figs 12-a and 12-b, respectively.

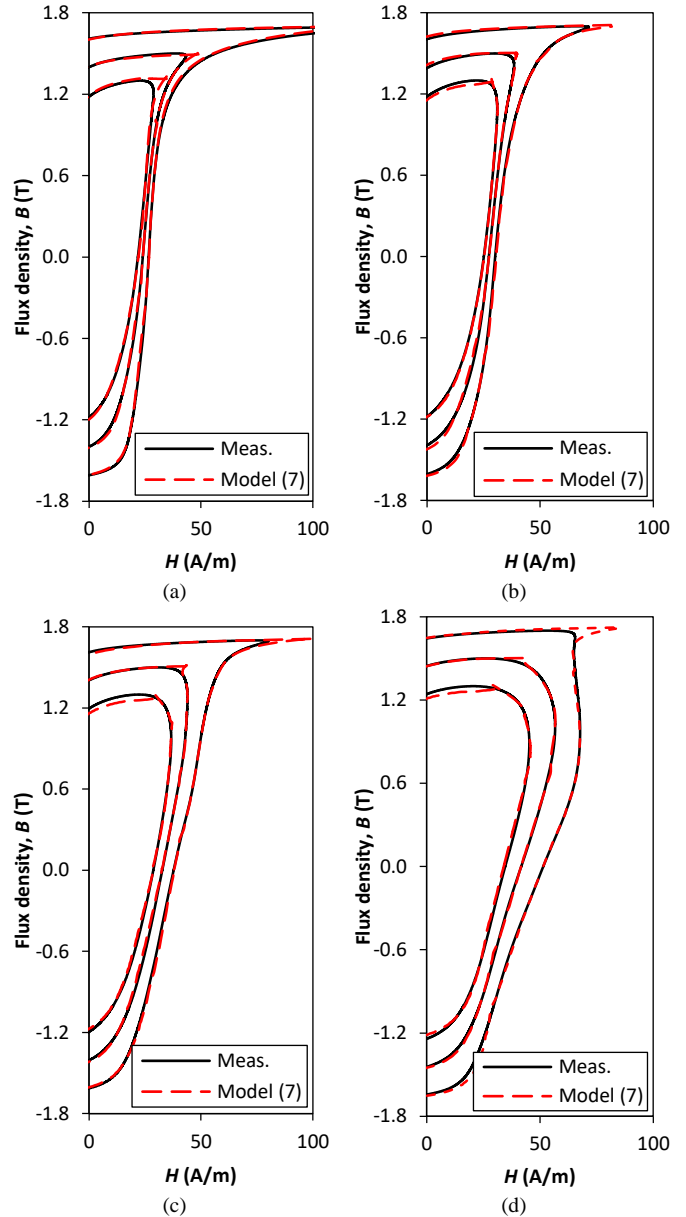


Fig 11 Comparison between the measured and modelled DHL at magnetising frequency of 50 Hz and peak flux densities of 1.3 T, 1.5 T and 1.7 T (a) pack # 1 (b) pack # 2 (c) pack # 3 and (d) pack # 4

Fig 12 shows a close agreement between the calculated and measured losses, with a maximum difference of less than 4 % for all flux densities, as shown in Fig 12-b. Therefore the developed models, based on the two terms model of (7), show a fairly accurate and reliable technique to reproduce the DHLs of magnetic cores subjected to ILFs, and hence for energy loss calculations and core quality assessment purposes.

For the designer of the electrical machines and transformers, it is of high importance to develop strategic skills and knowledge to safeguard the magnetic cores against ILFs at the design stage. The developed model can provide a reliable figure of effects of typical ILFs on the magnetising processes, energy loss and energy loss components of magnetic cores with GO materials.

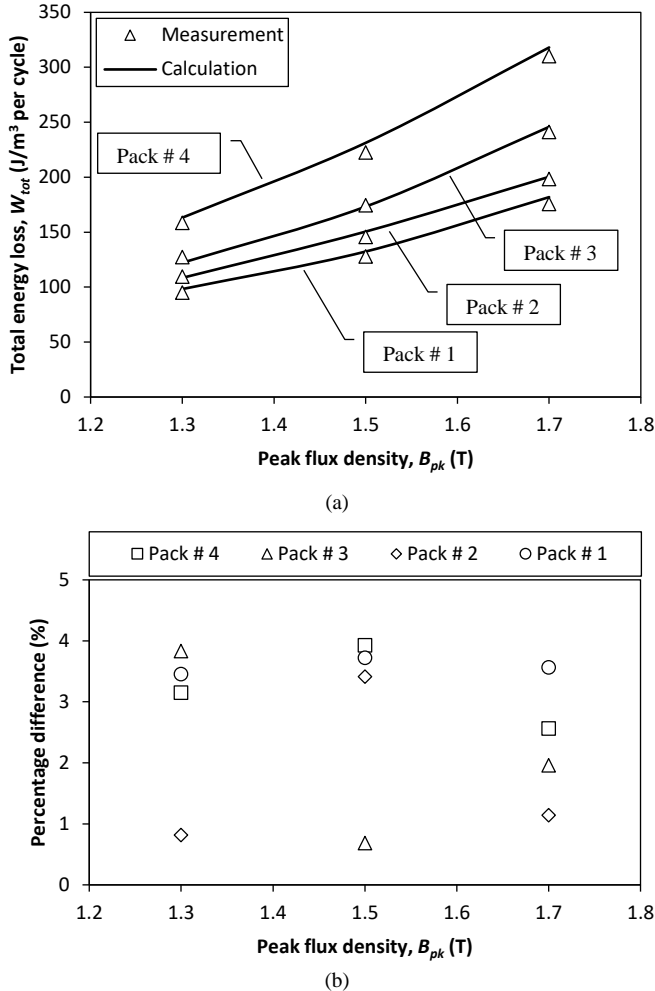


Fig 12 (a) Comparison between the calculated and measured energy losses
(b) Percentage difference between the calculated and measured values

VI. CONCLUSION

ILFs have been identified as a major threat for normal operation of magnetic cores of power transformers, electrical machines and other magnetic devices with laminated cores. Therefore, in the design of the magnetic cores for modern applications, it is important to study the impacts of ILFs on performance of the machine over the nominal range of frequency and flux density. In this paper a new approach was developed to condition monitoring and quality assessment of magnetic cores with GO materials. The study was performed based on the measured SHLs and DHLs. The results showed that core quality assessment can be effectively performed by monitoring and analysing the DHLs of the cores. The analysis can be completed for energy loss separation purposes by

additional measurements on the SHLs. This is an effective technique to monitor the overall condition of the magnetic cores.

A new analytical approach was also developed to reproduce the DHLs of the magnetic cores with ILFs. The accuracy of the method was validated on stacks of four laminations subjected to different kinds of ILFs. A close agreement, with a maximum difference of less than 4 %, was found between the calculated energy loss obtained from the developed approach and bulk measurements. The developed models can be implemented to evaluate typical ILFs on the hysteresis performance and total energy loss of magnetic cores of real power transformers and other magnetic devices with GO material.

ACKNOWLEDGMENT

The author is grateful to Cogent Power Ltd. for providing the electrical steel sheets, and Wolfson centre for magnetics at Cardiff University for the experimental work.

REFERENCES

- [1] H. Hamzehbahmani, P. Anderson, and K. Jenkins, "Inter-laminar Insulation Faults Detection and Quality Assessment of Magnetic Cores Using Flux Injection Probe", IEEE Trans on Power Delivery, Vol. 30, No. 5, October 2015, pp. 2205-2214
- [2] H. Hamzehbahmani, P. Anderson, K. Jenkins, and M. Lindenmo, "Experimental Study on Inter-Laminar Short Circuit Faults at Random Positions in Laminated Magnetic Cores", IET Electric Power Applications, Vol. 10, Issue 7, August 2016, pp. 604-613
- [3] S. Shah, O. Osemwinyen, P. Rasilo, A. Belahcen, A. Arkkio, "Thermographic Measurement and Simulation of Power Losses Due to Interlaminar Contacts in Electrical Sheets", IEEE Transactions on Instrumentation and Measurement, Vol. 67, No. 11, pp. 2628-2634, 2018
- [4] L. Masisi, M. Ibrahim, and J. Wanjiku, "The Effect of Two- and Three-Level Inverters on the Core Loss of a Synchronous Reluctance Machine", IEEE Trans. Ind. Appl., Vol. 52, No. 2, Sep. 2016, pp. 3805-3813
- [5] D. Bertenshaw, C. Ho, A. Smith, M. Sasi, and T. Chan, "Electromagnetic modelling and detection of buried stator core faults" IET Electric Power Applications, Vol. 11, Issue 2, March 2017, pp. 187-196
- [6] D. Bertenshaw, J. Lau, and D. Conley, "Evaluation of EL CID Indications not associated with Stator Core Inter-laminar Insulation Faults" IEEE Electrical Insulation Conference, June 2011, pp 254- 260
- [7] Y. Zhang, H. Wang, K. Chen and S. Li, "Comparison of laser and TIG welding of laminated electrical steels", Journal of Materials Processing Technology, Vol. 247, Sep. 2017, pp 55-63
- [8] S. Lee, G. Kliman, M. Shah, D. Kim, T. Mall, K. Nair, and M. Lusted, "Experimental Study of Inter-laminar Core Fault Detection Techniques based on Low Flux Core Excitation" IEEE Trans on Energy Convers, Vol. 21, No. 1, March 2006, pp 85-94
- [9] K. Bourchas, A. Stening, J. Souldard, A. Broddefalk, M. Lindenmo, M. Dahlen and F. Gyllensten, "Quantifying effects of cutting and welding on magnetic properties of electrical steels", IEEE Trans. Ind. Appl., Vol. 53, No. 5, pp. 4269-4278, Sep./Oct. 2017
- [10] H. Weiss, P. Tröber, R. Golle, S. Steentjes, N. Leuning, S. Elfgen, K. Hameyer, and W. Volk "Impact of Punching Parameter Variations on Magnetic Properties of Nongrain-Oriented Electrical Steel", IEEE Trans. on Ind. App., Vol. 54, No. 6, pp. 5869-5878, Nov., Dec. 2018
- [11] C. Ho, D. Bertenshaw, A. Smith, T. Chan, and M. Sasic "Three-dimensional finite element analysis of large electrical machine stator core faults", IET Electr. Power Appl., Vol. 8, No. 2, pp. 60-67, 2014
- [12] G. Kliman, S. Lee, M. Shah, R. Lusted and N. Nair "A new method for synchronous generator core quality evaluation," IEEE Trans. Energy Convers., Vol. 19, NO. 3, , Sep. 2004, pp. 576-582
- [13] R. Mazurek, H. Hamzehbahmani, A. Moses, P. Anderson, F. Anayi and T. Belgrand "Effect of Artificial Burrs on Local Power Loss in a Three-Phase Transformer Core" IEEE Trans Mag Vol 48, No 4, Apr 2012, pp 1653-1656
- [14] H. Hamzehbahmani, A. Moses and F. Anayi "Opportunities and Precautions in Measurement of Power Loss in Electrical Steel Laminations

- Using the Initial Rate of Rise of Temperature Method*" IEEE Trans. Mag. Vol. 49, No. 3, March 2013, pp 1264- 1273
- [15] H. Hamzehbahmani, P. Anderson, J. Hall, and D. Fox "Eddy Current Loss Estimation of Edge Burr Affected Magnetic Laminations Based on Equivalent Electrical Network-Part I Fundamental Concepts", IEEE Trans. on Power Delivery, Vol. 29, No. 2, April 2014, pp. 642-650
- [16] C. Schulz, S. Duchesne, D. Roger and J. Vincent "Short Circuit Current Measurements between Transformer Sheets", IEEE Trans Magn, Vol. 46, No. 2, Feb 2010, pp 536-539
- [17] G. Bertotti and I. Mayergoyz "The Science of Hysteresis", Academic Press 2005
- [18] S. Zirka, Y. Moroz, P. Marketos, A. Moses and D. Jiles "Measurement and modeling of B-H loops and losses of high silicon non-oriented steels", IEEE Trans. Magn., Vol. 42, No. 10, pp. 3177-3179, 2006
- [19] S. Zirka, Y. Moroz, N. Chiesa, R. Harrison and H. Høidalen "Implementation of Inverse Hysteresis Model Into EMTP—Part II: Dynamic Model", IEEE Trans On Power Delivery, Vol. 30, No. 5, pp 2233-2241, Oct 2015
- [20] S. Zirka, Y. Moroz, S. Steentjes, K. Hameyer, K. Chwastek, S. Zurek and R. Harrison "Dynamic magnetization models for soft ferromagnetic materials with coarse and fine domain structures", Journal of Magnetism and Magnetic Materials, Vol. 394, pp 229-236, Nov. 2015
- [21] S. Zirka, Y. Moroz, P. Marketos, and A. Moses "Viscosity-based magnetodynamic model of soft magnetic materials", IEEE Trans. Magn., Vol. 42, No. 9, pp. 2121-2132, Sep. 2006
- [22] C. Martinez, S. Jazebi and F. Leon "Experimental parameter determination and laboratory verification of the inverse hysteresis model for single-phase toroidal transformers", IEEE Trans. on Magn., Vol. 52, No. 11, Nov. 2016
- [23] O. Barrière, C. Ragusa, C. Appino and F. Fiorillo "Prediction of energy losses in soft magnetic materials under arbitrary induction waveforms and DC bias", IEEE Trans. Ind. Elec., Vol. 64, No. 3, pp. 2522-2529, Mar. 2017
- [24] H. Hamzehbahmani, P. Anderson and S. Preece "An application of an Advanced Eddy Current Power Loss Modelling to Electrical Steel in a Wide Range of Magnetising Frequency" IET Science, Measurement & Technology, Vol. 9, Issue 7, October 2015, pp. 807-816
- [25] G. Bertotti "General properties of power losses in soft ferromagnetic materials", IEEE Trans. Magn., Vol. 24, No. 1, pp. 621-630, 1988
- [26] H. Hamzehbahmani, "Development of a New Approach to Core Quality Assessment of Modern Electrical Machines", IET Electric Power Applications, Vol. 13, Issue 6, June 2019, pp. 750–756
- [27] BS EN 10280:2001 + A1:2007, *Magnetic Materials - Methods of measurement of the magnetic properties of electrical sheet and strip by means of a single sheet tester*, British Standard, 2007
- [28] UKAS M3003, "The Expression of Uncertainty and Confidence in Measurement," 1997
- [29] IEEE Guide for Diagnostic Field Testing of Electric Power Apparatus-Electric Machinery, IEEE Standard 62.2-2004, Jun. 2005

BIOGRAPHY



H. Hamzehbahmani received the BEng and MEng degrees in electrical engineering in 2005 and 2007, respectively; and PhD degree in electrical engineering from Cardiff University, UK in 2014. Between 2005 and 2010 he worked on distribution networks and HV substations as a consultant engineer. Following his PhD he was appointed as a research associate at Cardiff University in the field of earthing systems for HVAC and HVDC systems. From 2016 to 2018 he was a lecturer in electrical engineering with Ulster University in UK. He is currently an assistant professor in electrical engineering at Durham University. His main research interest includes magnetic materials and applications, power loss analysis and condition monitoring of transformers and electrical machines, high frequency and transient response analysis of earthing systems, earthing design of HVDC networks.